Chapter 11
A 13,000-Yr Record of Environmental Change from Tschuchye Lake in Northeast Yakutia

S. S. Burnatny, A. N. Naumov and Yu. A. Korzun

Abstract Tschuchye Lake is located in the central part of the Oimyakon Upland in eastern Yakutia (63.351465°N, 140.990055°E). A multi-proxy investigation of a sediment core from the lake provides evidence of abrupt changes in paleolimnological conditions during the Holocene. The chronology of the 347 cm lacustrine sediment sequences is delimited by four AMS ^{14}C ages from plant macrofossils. Three distinct lithological units are identified marking changes in sedimentation. Four pollen zones represent shifts in biocoenosis during the Holocene. Clear geochemical zonation occurs in the core. Coarse detrital material represented by silty sand and sandy silt are characterized by (1) low content of TiO_2, Al_2O_3, MgO, K_2O, Rb, Fe_2O_3, and LOI; (2) high content of SiO_2, Zr and Sr; and (3) low values of magnetic susceptibility, saturation magnetization, and saturation remanence. Laminated silt shows the highest content of Fe_2O_3, P_2O_5, MnO, MS, Jrs and Js, which implies autigenic or diagenetic processes. Magnetic particles are predominantly single domain, superparamagnetic and rarely multi domain and possibly are of bacterial origin.

Keywords Holocene · Lacustrine sediments · Rock magnetism
Inorganic geochemistry · Palynology

Introduction

Lacustrine sediments represent one of the best archives for paleoenvironmental information because of their continuous deposition and low-level of disturbance. Multidisciplinary research on lakes in central and eastern Yakutia has rarely been conducted and has focused so far on palynology and vegetation reconstruction (Andreev et al. 1997; Anderson et al. 2002). The use of magnetic and geochemical

S. S. Burnatny (✉) · A. N. Naumov · Yu. A. Korzun
North East Interdisciplinary Scientific Research Institute n.a.
N.A. Shilo of FEB RAS, 16, Portovaya St, Magadan, Russia 685000
e-mail: tesfarkon@gmail.com

D. Nurgaliev et al. (eds.), *Recent Advances in Rock Magnetism, Environmental Magnetism and Paleomagnetism*, Springer Geophysics,
https://doi.org/10.1007/978-3-319-90437-5_11

properties of lake sediments for interpreting environmental changes in this region has received less attention, although they are widely used as environmental proxies (Boyle 2002; Evans and Heller 2003; King and Peck 2002). In summer 2005, two lakes, Tschuchye and Ulu, were cored in eastern Yakutia. In addition standard palynological analyses, the sediments of Tschuchye Lake were studied to examine the variability and the origin of sediment magnetic and geochemical properties, with the aim to evaluate their sensitivity and usefulness for environmental reconstructions, to assess the relationship of biotic and abiotic indicators and the natural environment.

Study Area

Lake Tschuchye is located in the Oimyakon Upland of eastern Yakutia between the Kobyuma and Suntar Rivers (Fig. 11.1). The lake has a length and width of 950 and 360 m, respectively. The maximum water depth is 6.1 m. The lake is connected with the larger Ulu Lake by a shallow channel. The lake has a shallow discharge into the Tiryakh-Yuryakh River. The distance between the both lakes is about 800 m.

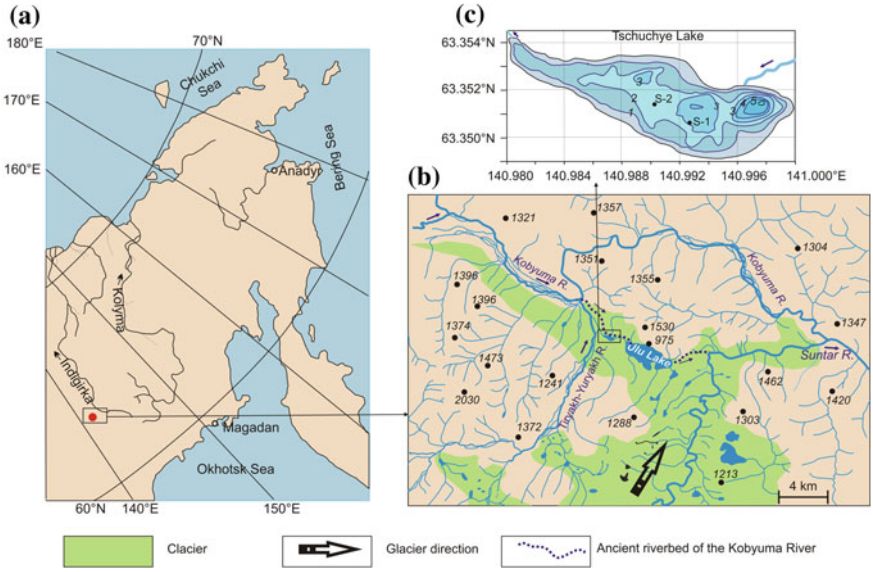

Fig. 11.1 Maps showing details of the study area, the location is indicated by the a red dot in a square in (**a**); drainage patterns, elevation, and locations of Tschuchye Lake (**b**); bathymetric map of Tschuchye Lake with depths shown in 1 m intervals (**c**). Coring locations are indicated on the bathymetric maps by a dark circle

Tschuchye and Ulu Lakes are of glacial origin. The glacier moved from the south along the valley of the Suntar River which originates on the northern slope of the Suntar-Hayat Range (Fig. 11.1). The damming effect of the glacier caused the ancient Kobyuma River to change direction. It is assumed that on the site of Tschuchye and Ulu lakes there is a buried river valley. Tschuchye and Ulu lakes are located in the moraine field. The deposits of the latter are distributed to the east and south of the lakes.

The climate of Oimyakon is subarctic with extremely severe and long winters, and only little precipitation (snow). The annual average January temperatures are—46.4 °C, and the annual average July temperatures are +14.9 °C. The absolute minimum winter and maximum summer temperatures measures are −65.4 and 34.6 °C, respectively.

The average annual humidity is 71% and the annual precipitation is 212 mm (http://www.pogodaiklimat.ru/climate/24688.htm).

The Oimyakon region is classified within the North Taiga subzone (Karaveav 1958). The light coniferous forest is dominated by *Larix cajanderi* Mayr. Other trees within the larch forests include birch (*Betula lanata* V. Vass., *B. platyphylla* Sucacz.), *Chosenia arbutifolia* (Pall.) A. Skvorts and poplar (*Populus suaveolens* Fisch.). The understory in the larch forests usually is a mix of *Betula middendorffii* Trautv. & C.A. Mey., *B. exilis* Sucacz., *Pinus pumila* (Pall.) Regel, various species of *Salix, Duschekia fruticosa* (Rupr.) Pouzar, *Rhododendron adamsii* Rehd., *Rh. parvifolium Adams*, Ledum.

Method

Two cores (Fig. 11.1) were taken in the central part of the Tschuchye Lake using a modified Livingstone piston sampler (Wright et al. 1984). Only the sediments of one core (S-1) were studied. Samples for rock magnetic analyses were cut every 1 cm from this core, yielding a total of 327 samples. The samples were dried at room temperature during a few days.

Mass-specific low-field magnetic susceptibility (MS) was measured on a MFK1-FA Kappabridge (AGICO Ltd., Brno, Czech Republic) having a sensitivity of 3×10^{-8} SI. Hysteresis parameters, including saturation magnetization (Js), induced magnetization (Ji), saturation remanence (Jrs), coercive force (Bc), and remanence coercivity (Bcr) were measured by an automatic coercive spectrometer (Burov et al. 1986). The sensitivities of remanent (Jr) and induced (Ji) magnetic moment are 1×10^{-8} Am^2 and 1×10^{-6} Am^2, respectively. The maximum specimen volume is 1.92 cm^3. The paramagnetic susceptibility (MSp) was recorded from the high-field slopes of the hysteresis curves.

The temperature-dependent susceptibility (MS-T) of the sediments was measured continuously from room temperature up to 700 °C and back to room temperature using a MFK1-FA Kappabridge equipped with a CS-3 high temperature furnace (AGICO Ltd., Brno, Czech Republic) having a sensitivity of 1×10^{-7} SI

and a maximum specimen volume of 0.25 cm^3. The heating and cooling rates were 10–12 °C min^{-1}. The samples were heated continuously from room temperature to 700 °C and then cooled back to room temperature in air, and for a few samples in argon. The Curie temperature was determined using the Hopkinson peaks and the temperature dependence of inverse susceptibility values (Lattard et al. 2006; Petrovský and Kapička 2006; Fabian et al. 2013).

Major and trace elements were analyzed in 95 samples using a S4 Pioneer X-ray fluorescence spectrometer (Bruker, Germany) and a VRA-30 XRF spectrometer (Germany). The elemental compositions were determined using the fundamental parameters method (Borkhodoev 2002). The relative content of organic material was estimated using loss on ignition (LOI) after heating the samples to 500 and 1000 °C (Heiri et al. 2001).

Palynological samples were prepared using standard procedures for organic-poor sediments (PALE 1994). A minimum of 300 known arboreal and non-arboreal pollen grains was identified in each sample. Pollen calculations and diagrams were done using Tilia and Tilia-graph (https://museum.state.il.us./pib/grimm/tilia). Pollen zonation was done qualitatively based on percentage changes in major taxa.

The ^{14}C dates were obtained from plant macrofossil samples and carried out at the Center for Accelerator Mass Spectrometry, Lawrence Livermore National Laboratory (USA). Radiocarbon and tephra dates were converted into calibrated ages with IntCal 13 (Reimer et al. 2013). An age-depth model was then constructed using Bacon (Blaauw and Christen 2011).

Micrographs of magnetic extract were obtained by D.V. Fomin in Far East Scientific Center (Vladivostok) using microscope SIGMA HD (Carl Zeiss Microscopy GMBH).

Lithology and Chronology

The sediments from core S-1 include three lithological units.

Unit 1 (315–347 cm) is composed of massive homogeneous sandy silt with layers (0.5-cm-thick) of sand between 320 and 325 cm.

Unit 2 (250–315 cm) is characterized by laminated silt. Layering is due to the alternation of light gray and gray silts. The unit includes layers of sandy silt (a, b, c, d) at 294–298, 274–275, 260–261, and 251–252 cm.

Unit 3 (0–250 cm) consists mainly of a homogeneous and massive gray silt. The unit includes layers (a, b, c, d, e) of silty sand at 213–225, 182–187, 112–124, 43–48, and 15–22 cm, as well as a tephra (1.5–2 mm thick) at 244 cm. The tephra is correlated with the 7600 ^{14}C-yearBP eruption of the Kurile Lake caldera on Kamchatka. It is a valuable stratigraphic marker for southern Kamchatka, the Sea of Okhotsk, and a large part of the northern Asian mainland, where it has been identified in terrestrial and lake sediments (Ponomareva et al. 2004).

The chronology of lake sediments is based on AMS ^{14}C dates and the Kuril tephra (Table 11.1) (Korzun 2017).

Table 11.1 Radiocarbon dating

Depth (cm)	Lab no.	14C age	Calibrated age	Material dated
101	CAMS 174,820	4315 ± 35	4900 ± 45	Plant macrofossil
143	CAMS 174,821	4955 ± 45	5690 ± 50	Plant macrofossil
187	CAMS 174,818	6140 ± 35	7060 ± 75	Plant macrofossil
244	Tephra	7650 ± 50	8465 ± 50	
329	CAMS 174,822	11,770 ± 30	13,665 ± 110	Plant macrofossil

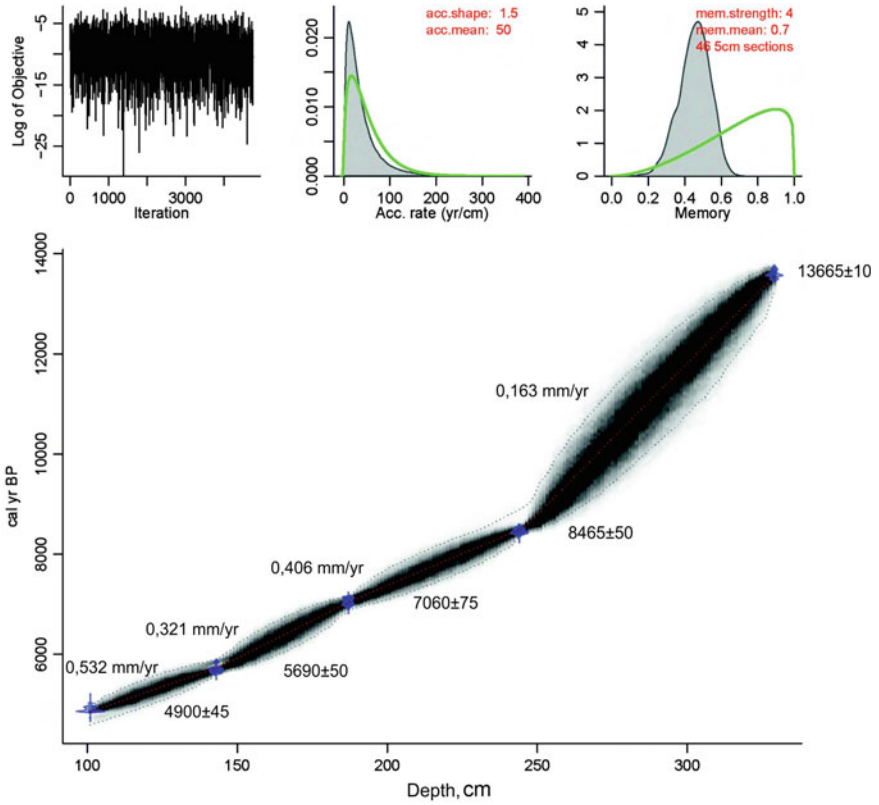

Fig. 11.2 Age-depth model for Tschuchye Lake sediments produced by the Bacon software package (Blaauw and Christen 2011). Dotted lines show the 95% confidence

Figure 11.2 shows age-depth model for Tschuchye Lake. Mean sedimentation rates were calculated for intervals between adjacent dates. The sedimentation rates vary from 0.163 to 0.532 mm/yr. The lowest sedimentation rate corresponds to unit 2, which is characterized by laminated silt.

Palynology

Four pollen zones trace the major changes in vegetation near Tschuchye Lake. The pollen concentration in the basal 12 cm of the core was too low for counting. One of the most striking characteristics of this record are the consistent and relatively high *Larix* pollen percentages. In contrast to many other pollen records from West Beringia, the Tschuchye data indicate the presence of tree environments since ~13,800 cal yr. BP.

Open *Larix* (larch) forests mixed with shrub *Betula* (birch) established exceptionally early (pollen zone TS1 ~13,800–13,300 cal yr BP), compared to other areas of northeastern Siberia and indicate warm, dry climates. Zone TS1 has the highest content of non-arboreal pollen, dominated by Poaceae, Cyperaceae, and *Artemisia*.

Between ~13,300–10,300 cal yr BP (zone TS2), *Larix* was more common and the forest understory supported abundant *Betula* and *Salix* (willow). Zone TS2 is marked by the rise in tree and shrub sums (up to 65%). *Salix* pollen has some of the highest values within the core.

Shrub *Alnus* (alder) became important in the region around 10,300 cal yr BP (zone TS3 ~ 10,300–6900 cal yr BP).

Pinus pumila (stone pine) was the last major taxa and occurred at ~6900 cal yr BP (zone TS4), perhaps being most abundant ~5600–4900 cal yr BP, and indicates conditions warmer and wetter than present.

The modern vegetation established ~700 yr ago.

Rock Magnetism

Shifts in the main magnetic properties of core S-1 closely correspond to lithological changes (Fig. 11.3). The layers of silty sand and sandy silt in Unit 2 (a, b, c, d) and Unit 3(a, b, c, d, e) are characterized by average values for MS (8.9×10^{-8} kg/m^3), Js (0.0045 Am^2/kg), and Jrs (0.0016 Am^2/kg). There are low and high values for the paramagnetic susceptibility.

The sediments of Unit 1, composed of sandy silt, show similar values for MS (9.67×10^{-8} kg/m^3), Js (0.0055 Am^2/kg), Jrs (0.0025 Am^2/kg), and MSp (5×10^{-8} kg/m^3) but have higher values for Bc (30.34 mT) and Bcr (54.16 mT). These magnetic zones are shown by colored bars in Fig. 11.3.

Sediments of Unit 2 are clearly distinguished in the core, because of their strong variations in magnetic parameters. The sediments are characterized by maximum average values for MS (23.8×10^{-8} kg/m^3), Js (0.019 Am^2/kg), and Jrs (0.0085 Am^2/kg). In contrast to Unit 1, Bc and Bcr correspond to enhanced values of MS, Js and Jrs.

The magnetic parameters of the sediments in the upper part of Unit 1, excluding the sandy layers, vary slightly throughout the unit: MS = 13.6×10^{-8} kg/m^3,

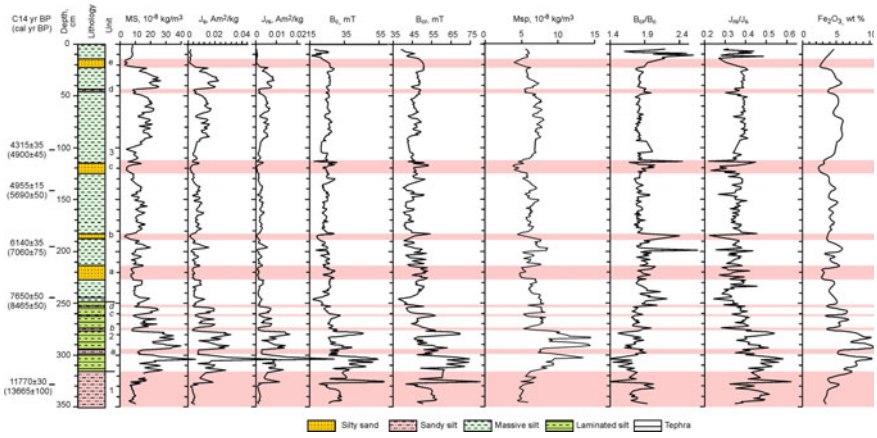

Fig. 11.3 Magnetic susceptibility (MS), saturation magnetization (Js), saturation remanence (Jrs), coercive force (Bc), remanence coercivity (Bcr), paramagnetic susceptibility (MSp), ratios Bcr/Bc, Jrs/Js, and Fe_2O_3 contents from core S-1 plotted versus depth. The lithological units described in the text are given to the right of the diagram

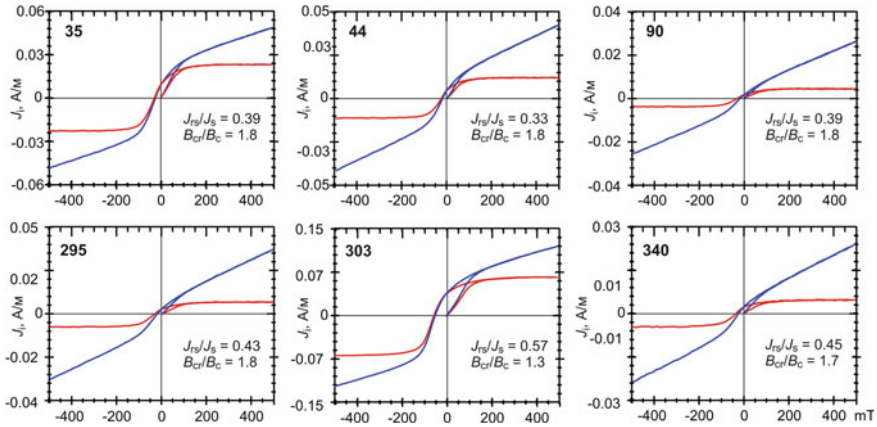

Fig. 11.4 Hysteresis loops of representative samples. The blue and red curves represent the data before and after the correction for the paramagnetic component, respectively. The sample numbers correspond to depths and are marked in bold font. Jrs/Js and Bcr/Bc ratios were calculated after correction for the paramagnetic component

Js = 0.0082 Am^2/kg, Jrs = 0.0030 Am^2/kg. Higher values of MS, Js and Jrs characterize the sediments from 20 to 100 cm.

Figure 11.4 shows hysteresis loops of representative samples. In all samples, the raw and dia/para-corrected loops are apparently different because of the paramagnetic or diamagnetic contributions. Higher diamagnetic/paramagnetic contributions are observed in silty sand (sample 340, 295) and sandy silt (sample 44).

Day-plot has been widely used to determine the domain state of magnetic minerals (Day et al. 1977; Dunlop 2002). The values of Jrs/Js and Bcr/Bc plotted on a Day diagram indicate that the domain state of magnetic minerals mixtures in the different lithological units from Tschuchye Lake varies (Fig. 11.5). The laminated sediments of Unit 2 (green rhombi symbols) plot predominantly in the SD area. Some samples from this unit are located near the SP-SD mixture curve, suggesting the presence of superparamagnetic particles.

The samples from sandy silt and silty sand (blue square symbols) are located in the lower part of the cluster between the SD-MD and SP-SD curves, but in an area above Jrs/Js = 0.2. These locations approximately correspond to a MD contribution of 20–40%. Samples from Unit 1 and Unit 3 plot predominantly between the SD-MD and SP-SD curves in the area Jrs/Js = 0.3–0.4, indicating the occurrence of SD, SP and MD particles.

High-Temperature Dependence of Magnetic Susceptibility

Selected samples of lacustrine sediments, tephra, and pebbles were subjected to susceptibility vs. temperature measurements in air. The temperature was increased continuously from room temperature to 700 °C and cycled back to 50 °C; some samples were measured in argon (Fig. 11.6).The behavior of the samples can be divided into four general types of thermomagnetic curves. All curves from the first heating run are irreversible.

The first type of curve shows a decrease in susceptibility up to the Curie points of magnetite at 580 °C, with a cooling curve that is much higher (Fig. 11.6k)

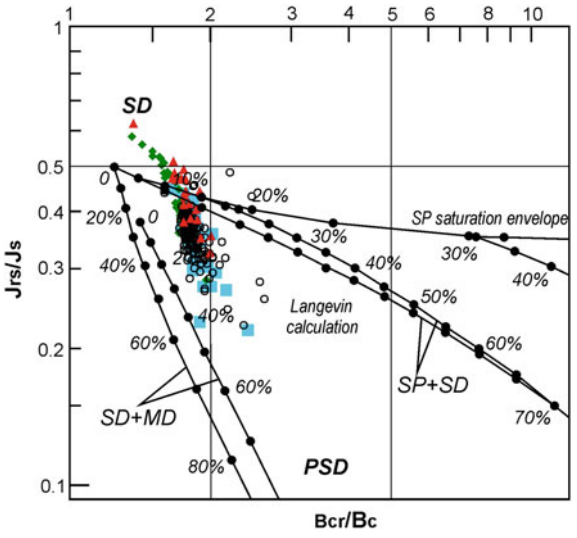

Fig. 11.5 The Day diagram for sediments of core S-1. SD, SP, PSD, and MD are single domain, superparamagnetic, pseudo-single domain, and multi domain particles, respectively. The SD–MD and SD–SP mixing lines with black dots refer to calculations from Dunlop (2002). The green rhombi, blue squares, red triangles, and open circles represent samples from laminated silt of Unit 2, and sandy silt and silty sand from Unit 1 and Unit 3, respectively

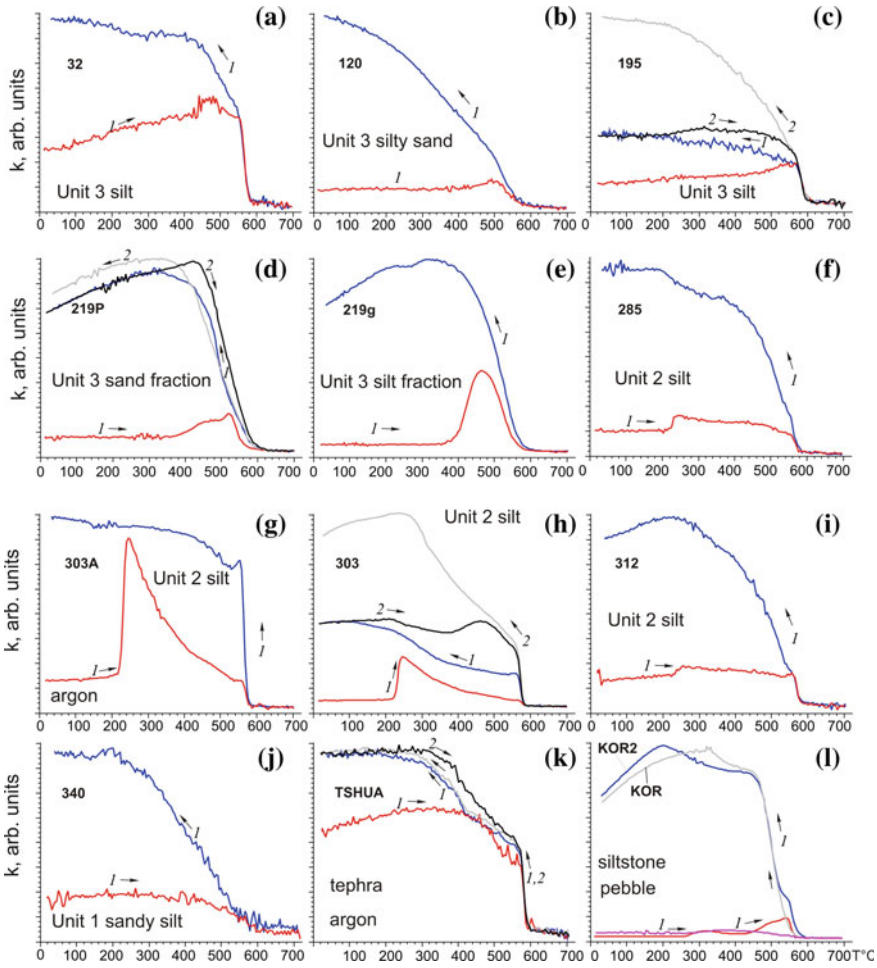

Fig. 11.6 Susceptibility versus temperature curves for sediments, tephra and rocks. The arrows and numbers in italic indicate the heating and cooling runs. Sample numbers are marked by bold font and correspond to depth

because of mineral neo-formation during heating. This newly formed mineral is also magnetite. This type of curve is characteristic of some samples from Unit 1.

The second type shows an increasing magnetic susceptibility at T ~220 °C, followed by a decrease during further heating to ~580 °C (Fig. 11.6f, h, i). Heating in argon also shows an increase in MS at T ~220 °C (Fig. 11.6g). This behavior supposedly is associated with the presence of lepidocrocite, which transforms into maghemite–hematite (Gehring et al. 1990; Gehring and Hofmeister 1994; Gendler et al. 2005; Hanesch et al. 2006). Upon cooling, increases in susceptibility are seen at the Curie temperature of magnetite. Such curves are typical for the laminated sediments of Unit 2.

The third type displays an increase in susceptibility at 380–420 °C and a sharp drop at 580 °C (Fig. 11.6a, b, c, d, e). Cooling curves all show a considerable increase in susceptibility starting at 580 °C. This type of curve reflects the influence of organic material on the transformation of Fe-bearing minerals, such as goethite, ferrihydrite and hematite (Hanesch et al. 2006) as well as biotite, vivianite, hypersthene (Minyuk et al. 2011). Sample 219 was divided into sand and silt fractions. Both fractions show an increase in susceptibility at 380 °C but with a sharper peak in MS for the silt fraction (Fig. 11.6d, e).

The forth type of curve characterizes the tephra (Fig. 11.6). The sample was heated in argon. The heating curve shows a small but distinct decrease near 547 °C and a sharp drop at ~590 °C, marking the presence of low-titanium magnetite and magnetite. The cooling curves display a strong increase in susceptibility at 425 °C, indicating the formation (transformation) of a new mineral. This mineral is stable. All curves of the second run are reversible.

Thermomagnetic curves from pebbles of siltstone and sandstone are variable. The second and third types of curves typify these samples (Fig. 11.6m). All samples finish with susceptibility hundreds of times higher than the initial values.

Inorganic Geochemistry

The geochemical characteristics of lacustrine sediments depend on many factors, including the: (1) chemical composition of the provenance; (2) physical and chemical weathering processes in the catchment area; (3) tectonic and eolian activity; (4) sorting during transport and sedimentation; and (5) post-depositional diagenetic changes (e.g. Fralick and Kronberg 1997).

Principal component analysis (PCA) was used to reduce the dimensions of the multivariate data set using the PAST software program (Hammer et al. 2001). This analysis was performed on a correlation matrix of major and trace elements, LOI and magnetic susceptibility.

The first PC axis explains 52% of the total variance. It is positively correlated with Al_2O_3, TiO_2, Fe_2O_3, MgO, Cr, Rb, Ba, MS, and LOI and negatively correlated with SiO_2, Zr, and Sr (Fig. 11.7). The second PC axis explains an additional 18% of the variability and is characterized by positive loadings of P_2O_5, MnO, MS, CaO, MS, Fe_2O_3, and LOI. It is negatively correlated with Al_2O_3, TiO_2, Cr, Ni, Rb, and Ba. These results indicate the presence of three main data groups. SiO_2, Sr, and Zr are clearly related to silty sand and sandy silt, where as Al_2O_3, TiO_2, Cr, Ni, and Ba correspond to silt. P_2O_5, MnO, MS, CaO, MS, Fe_2O_3, and LOI are associated with sediments of high authigenic processes and post-depositional diagenetic changes.

The elemental record from core S-1 can be divided into two groups or geochemical zones based on the variability of the inorganic compounds and LOI (Figs. 11.8 and 11.9). These zones coincide with the rock magnetic zones. Different environmental conditions are reflected in the variations in the sediment deposition. Sandy silt and silty sand (colored bars in Figs. 11.8 and 11.9) represent dynamic

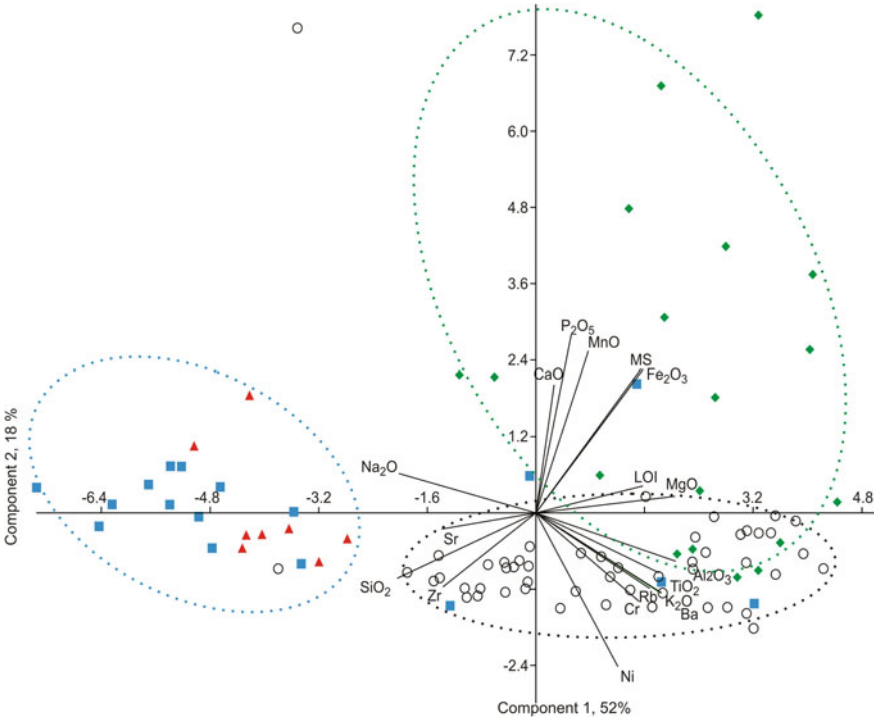

Fig. 11.7 Principal component analysis of the Tschuchye Lake sediments. Green rhombi, blue squares, red triangles, and open circles represent samples from laminated silt of Unit 2, sandy silt and silty sand from Unit 1 and Unit 3, respectively

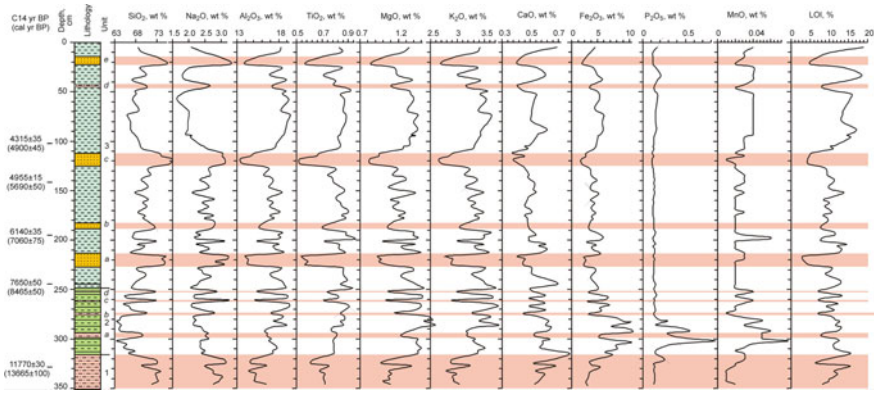

Fig. 11.8 Graphs of major elements plotted versus depth

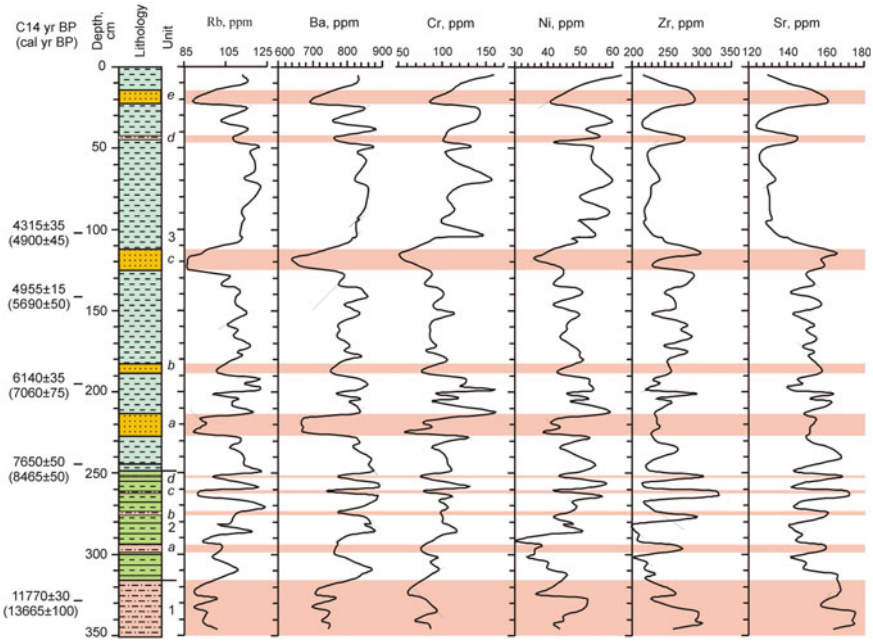

Fig. 11.9 Graphs of trace elements plotted versus depth

facies and reflect a high input to the lake basin of coarse detrital material. It was noted that coarse detrital sediments, such as sand, are enriched with SiO_2, Sr, and Zr and have low LOI. These sediments have a low TiO_2/Zr index, indicating dynamic sorting of the material (Yudovich and Ketris 2011). Petrographic analyses of thin sections of the sand indicate the presence of quartz, feldspar and siltstone-sandstone grains. In turn, siltstone-sandstone grains consist of quartz, feldspar and clay minerals.

The laminated silt of Unit 2 shows wide-scale variations in elemental content. The sediments are enriched in Fe_2O_3, P_2O_5, and MnO, showing similar patterns of variation throughout the core. These elements are apparently associated with the accumulation of an iron-manganese crust. Phosphorus is related partially to manganese in oceanic sediments, in particular, occurring in ferromanganese nodules (Sevast'yanova 1981, 1982). Iron-manganese nodules are often formed when the sedimentation regime changes under oxic conditions (Yudovich and Ketris 2011). In El'gygytgyn and Grand lakes of northeastern Siberia, the presence of phosphorus and manganese is related partly to vivianite (Minyuk et al. 2014; Minyuk and Borkhodoev 2016). Values of LOI widely oscillate throughout the core, with highest values between 0 and 100 cm, which reflects the high organic content in this part of the record.

Discussion

The very low values of the magnetic parameters that characterize the sediments of Tschuchye Lake reflect the low magnetic properties of the catchment material. The main input into the lake comes from Permian sedimentary rocks, located along the northern shore, and moraine deposits from the southern and eastern shores of the lake. The magnetic susceptibility of the pebbles (18 samples) collected near the lake has low values—3.3–10.8 (5.6) $\times$ 10^{-8} kg/m^3, which are comparable with the MS of sandy silt and silty sand (average of 8.9 $\times$ 10^{-8} kg/m^3). Regarding the Tschuchye Lake, low magnetic properties of the sediment mark an intense influx of coarse detrital material enriched with quartz and feldspars; thus mainly dia- and paramagnetic minerals which explain the low susceptibility, Js and Jrs values. The presence of sandy silt and silty sand layers is apparently associated with flood events.

The magnetic parameters of sediments correlate with the content of total iron. A positive correlation exists between MS, Js, Jrs and MSp with iron (Fig. 11.10). This is the first lake from the northeastern Siberia, where this pattern is revealed. In other lakes from this region (e.g., Lake El'gygytgyn, Chukotka (Minyuk et al. 2014), Lake Grand, northern Priokhotye (Minyuk and Borkhodoev 2016) no correlation of the iron content with the MS, Js, Jrs is observed. The main source of iron in the sediments of those lakes is in the paramagnetic minerals. The content of total iron is lower in coarse, weakly magnetic detrital material and higher in silt in the sediments of Tschuchye Lake, suggesting that iron influx to the basin is primarily due to clay particles and organic matter (Davison 1993). Silt enriched with Fe_2O_3, Al_2O_3, TiO_2, MgO, and increased LOI, which agrees with the geochemical data on the study of various granulometric fractions of the diluvium near Lake Grand,

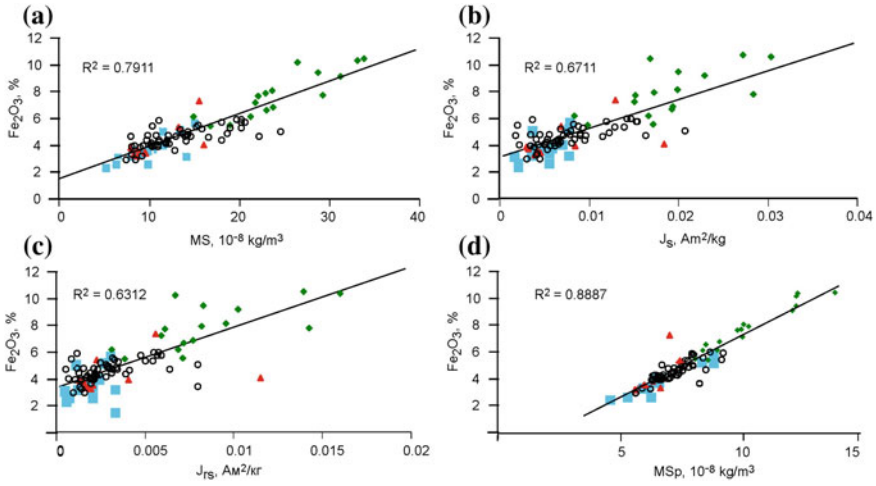

Fig. 11.10 Fe_2O_3–MS, Fe_2O_3–Jrs, Fe_2O_3-Js, Fe_2O_3-MSp diagrams for sediments

where silt and clay fractions also are enriched in these elements (Minyuk and Borkhodoev 2016).

The iron in the sediment is structure-bound in clay minerals and/or forms amorphous iron hydroxide that available for reduction to ferrous iron (Davison 1993). High positive correlations occur between Fe_2O_3 and MgO (r = 0.79), TiO_2 and MgO (r = 0.76) suggesting that part of iron is associated with the presence of chlorite ($Mg_{3.5}Fe_{1.5}Al_2Si_3O_{14}$) (Boyle 2002), or biotite ($K_{0.9}Na_{0.01}$)($Mg_{1.5}$ Fe1.1) ($Al_{0.05}Ti_{0.2}$) [$Si_{2.9}Al_{1.1}O_{10}$]$(OH)_2$ (e.g., Just and Kontny 2012).

The strong positive correlation between Fe_2O_3 and MS (r = 0.89) indicates that part of the iron is incorporated also into detrital or/and chemical (biogenic) ferromagnetic minerals.

Because of the high mineralogical transformations during heating, it is not possible to determine the composition of detrital magnetic minerals by the thermomagnetic method. On the other hand, the extremely low magnetic properties of sediments do not allow us to separate the magnetic extract for mineralogical study. Magnetite was determined in some samples from Unit 1, where there were no new magnetic minerals formed during heating.

Hysteresis data indicate the dominance in sediments of single-domain and superparamagnetic particles. Micrographs of magnetic extract from sediment of Unit 2 (depth 303 cm) show the needle-like morphology particles and rounded shape particles, that are interpreted as lepidocrocite and magnetite, respectively (Fig. 11.11) (Webster et al. 2012; Song et al. 2015). The size of the rounded particles is up to several tens of nanometers as reported for synthesized abiotic and biotic magnetite (e.g. Li et al. 2013).

Principal component analysis shows that MS, Fe_2O_3, MnO, and P_2O_5 form a separate cluster on the PCA diagram (Fig. 11.7). The positive correlations between Fe_2O_3 and P_2O_5 (r = 0.67), Fe_2O_3 and MnO (r = 0.63), P_2O_5 and MnO (r = 0.64) are supposed to be caused by the formation of autigenic Fe–Mn oxyhydroxides or/and vivianite ($Fe_3(PO_4)_2$ $8H_2O$). Visible vivianite as a blue spots was found in the sediments of Unit 2 and Unit 3. Sediments from Unit 2, enriched with Fe_2O_3, MnO, P_2O_5, include also lepidocrocite.

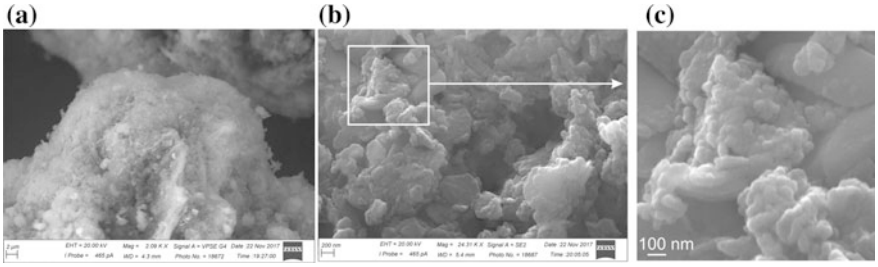

Fig. 11.11 Micrographs of magnetic extract from the sediments of Unit 2: **a** lepidocrocite?, **b**, **c** magnetite?

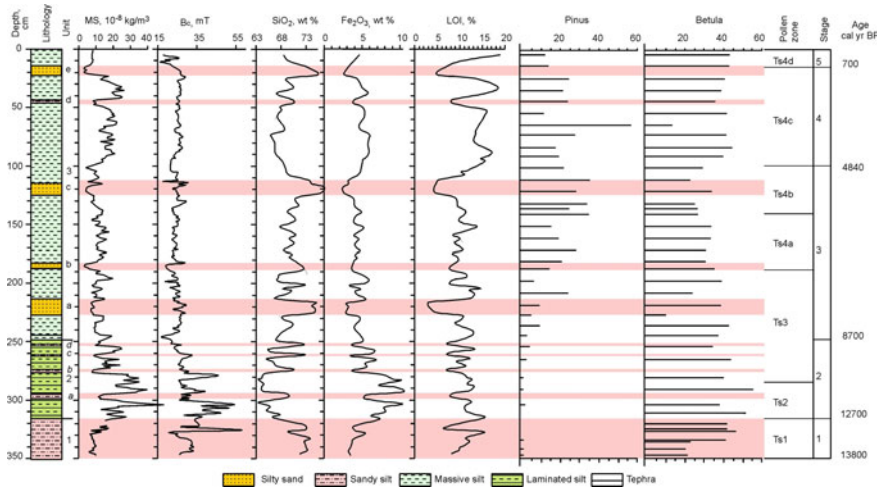

Fig. 11.12 Selected rock magnetic, geochemical, and palynological proxies plotted versus depth

The magnetic and geochemical characteristics, lithological units, and palynological zones indicate that the palaeolimnological and palaeoenvironmental history of Tschuchye Lake can be divided into five stages (Fig. 11.12).

Stage 1, 13,800–12,700 cal. yr BP. This stage marks initial formation of the lake following climate warming, glacial degradation and establishment of open *Larix* forest-*Betula* shrub tundra in the valley. This interval is also characterized by dynamic sedimentation within the Tschuchye basin, which is associated with an input of weak magnetic (low MS, Js, Jrs) detrital material that is enriched in quartz, feldspars, and clay minerals. High values of Bc and Bcr reflect the accumulation of Fe-oxyhydroxides.

Stage 2, 12,700–8780 cal yr BP. During this stage, the core lithology changes to laminated silt, which suggests seasonal variations in sedimentation. The accumulation of coarse material decreases from the previous stage, reflecting a decline in erosion within the catchment area. During this interval, the climate was likely as warm as or warmer than in present times, but relatively dry. *Larix* forest was common with abundant *Betula* and *Salix*. *Alnus* became a major landscape component ~11,200 cal yr BP. The high contents of iron, phosphorus and manganese indicate the occurrence of intensive digenetic and autigenic processes and the possible accumulation of a Fe–Mn crusts and of lepidocrocite. These results suggest that oxic conditions characterized the lake. The lowest contents of Zr and SiO_2 in laminated silt suggest the decreasing of detrital input to the lake. High values of MS, Jrs, Js, Bcr, Bc, and Jrs/Js indicate the presence of predominantly single domain particles, possible, of magnetite of chemical or bacterial origin. In most cases, magnetite-producing magnetotactic bacteria were found in and above the oxic-anoxic transitional zone (Bazylinski, 1996).

Stage 3, 8700–4840 cal yr BP. *Pinus pumila* became more common in the landscape during this interval, indicating of wetter climate with increased winter precipitation as snow. Maximum *Pinus pumila* percentages occur between 5655 and 4840 cal yr BP. During this interval, the values of MS, Jrs, and Js are low, whereas SiO_2, Sr, Rb are enhanced, reflecting an increased input of coarse detrital material into the basin. This pattern seems consistent with more intense slope erosion related to an increase in spring snow-melt.

Stage 4, 4840–700 cal yr BP. Although *Betula* and *Pinus* pollen percentages are variable during this period, the general trends suggest that *Betula* was more and *Pinus pumila* less common than during the previous stage. Spring erosion and input of coarse material into the lake were reduced. Consequently, sediments are relatively high in MS, Jrs, and Js. Stage 4 is characterized by high accumulation of organic matter, except for levels dominated by sandy silt and silty sand. In comparison with the previous stage, there are considerable increases in the accumulation of iron, phosphorus and manganese, suggesting an intensification of diagenetic and authigenic processes but less than during stage 2. The accumulation of Cr and Ni is also increased. Possibly these elements were absorbed by organic matter indicating an increase in biological production in the basin (e.g., Sharma et al. 2004).

Stage 5, 700–0 yr BP. This stage is characterized by the establishment of the modern vegetation. It is also characterized by the highest accumulation of organic matter but with a low input of coarse detrital material (low content of SiO_2). The values of MS, Jrs, Js are decreasing, presumably due to dilution by organic matter, while the contents of Cr and Ni are increased.

Conclusion

A multi-proxy investigation of a sediment core from Tschuchye Lake provides evidence of abrupt changes in limnological conditions during the Holocene.

Three distinct lithological units are identified, marking changes in sedimentation.

Coarse detrital material is characterized by (1) low content of TiO_2, Al_2O_3, MgO, K_2O, Rb, and Fe_2O_3, and low LOI values; (2) high content of SiO_2, Zr and Sr; and (3) low values of magnetic susceptibility, saturation magnetization, and saturation remanence.

Laminated silt shows the highest content of Fe_2O_3, P_2O_5, MnO, MS, Jrs and Js, which implies the occurrence of autigenic or diagenetic processes. The magnetic mineral grain size fraction consists predominantly of single domain, super-paramagnetic and rarely of multi domain and possibly are of bacterial origin.

Five stages of paleolimnological and paleoenvironmental history of Tschuchye Lake are defined based on the above changes.

Acknowledgements These studies were funded by the Far East Branch Russian Academy of Sciences (15-I-2-067).

References

Anderson, P.M., Lozhkin, A.V. & Brubaker, L.B. Implications of a 24,000-yr palynological record for a Younger Dryas cooling and for boreal forest development in Northeastern Siberia. Quaternary Research. 2002. Vol. 57. P. 325–333.

Andreev, A.A., Klimanov, V.A. & Sulerzhitsky, L.D. Younger Dryas pollen records from central and southern Yakutia. Quaternary International. 1997. Vol. 41/42. P. 111–117.

Bazylinski, D.A. Controlled biomineralization of minerals by magnetotactic bacteria. Chemical Geology. 1996. Vol. 132. P. 191–198.

Blaauw, M. and Christen, J.A. Bacon Manual. 2011. Vol. 2.2. http://www.chron.qub.ac.uk/blaauw/bacon.html.

Borkhodoev, V. Ya. Accuracy of the fundamental parameter method for x-ray fluorescence analysis of rocks. X-Ray Spectrom. 2002. Vol. 31. P. 209–218.

Boyle, J. F. Inorganic geochemical methods in paleolimnology, in: Tracking Environmental Change Using Lake Sediments Volume 2: Physical and Geochemical Methods, edited by: Last, W. M. and Smol, J. P., Springer, Berlin, 2002. P. 83–141.

Burov, B.V., Nurgaliev, D.K., and Yasonov, P.G., Paleomagnitnyi analiz (Paleomagnetic Analysis), Kazan: KGU, 1986 (in Russian).

Davison, W. Iron and manganese in lakes. Earth Sci. Rev. 1993. Vol. 34. P. 119–163.

Day, R., Fuller, M., and Schmidt, V.A. Hysteresis Properties of Titanomagnetites: Grain_Size and Compositional Dependence. Phys. Earth Planet. Inter. 1977. Vol. 13. P. 260–267.

Dunlop, D.J. Theory and application of the Day plot (*M*rs/*M*s versus *H*cr/*H*c) 1. Theoretical curves and tests using titanomagnetite data. J. Geophys. Res. 2002. Vol. 107. P.56–60.

Evans, M.E. and Heller, F. Environmental Magnetism. Principles and Applications of Enviromagnetics, edited by Dmowska R., Holton J.R., and Rossby H.T. Academic Press. 2003. 299 p.

Fabian, K., Shcherbakov, V.P., and McEnroe, S.A. Measuring the Curie temperature. Geochem. Geophys. Geosyst. 2013. Vol. 14. P. 947–961.

Fralick, P.W., Kronberg, B.I. Geochemical discrimination of elastic sedimentary rock sources. Sedimentary Geology. 1997. Vol. 113. P. 111–124.

Gehring, A.U. and Hofmeister, A.M. The Transformation of Lepidocrocite during Heating: a Magnetic and Spectroscopic Study. Clays Clay Miner. 1994. Vol. 42. P. 409–415.

Gehring, A.U., Karthein, R., and Reller, A. Activated State in the Lepidocrocite Structure during Thermal Treatment. Naturwissenschaften. 1990. Vol. 77. P. 177–179.

Gendler, T.S., Shcherbakov, V.P., Dekkers, M.J., Gapeev, A.K., Gribov, S.K., and McClelland, E. The Lepidocrocite-Maghemite-Haematite Reaction Chain: I. Acquisition of Chemical Remanent Magnetization by Maghemite, Its Magnetic Properties and Thermal Stability. Geophys. J. Int. 2005. Vol. 160. P. 815–832.

Hammer, Ø., Harper, D. A. T., and Ryan, P. D. PAST: Paleontological statistics software package for education and data analysis Palaeontol. Electron. 2001. Vol. 4. 9 pp.

Hanesch, M., Stanjek, H., and Petersen, N. Thermomagnetic Measurements of Soil Iron Minerals: the Role of Organic Carbon. Geophys. J. Int. 2006. Vol. 165. P. 53–61.

Heiri, O., Lotter, A. F., and Lemcke, G. Loss on ignition as a method for estimating organic and carbonate content in sediments: reproducibility and comparability of results. J. Paleolimnol. 2001. Vol. 25. P. 101–110.

Just, J. and Kontny, A. Thermally induced alterations of minerals during measurements of the temperature dependence of magnetic susceptibility: a case study from the hydrothermally altered Soultz-sous-Forêts granite, France. Int. J. Earth Sci. 2012. Vol. 101. P. 819–839.

Karavaev, M.N. Synopsisof the Flora of Yakutia. USSRAcademy of Sciences, Moscow-Leningrad, 1958 (In Russian).

King, J and Peck, J. Use of palaeomagnetism in studies of lake sediments. In Tracking Environmental Change Using Lake Sediments Volume 1: Basin Analysis, Coring, and Chronological Techniques, edited by: Last, W. M. and Smol, J. P., Springer, Berlin, 2002. P. 371–389.

Korzun, Ju. A Palynological analysis of glacial lake sediments from the upper basin of the Indigirka River. Bulletin of the North-East Scientific Center, RussianAcademy of Sciences Far East Branch. 2017. Vol. 1. P. 24–31 (In Russian).

Lattard, D., Engelmann, R., Kontny A. and Sauerzapf, U. 2006. Curie temperatures of synthetic titanomagnetites in the Fe-Ti-O system. Reassessment of some methodological and crystal chemical effects. J. Geophys. Res. 2006. Vol. 111, B12S28.

Li, J., Benzerara, K., Bernard, S., Beyssac, O. The link between biomineralization and fossilization of bacteria: Insights from field and experimental studies. Chemical Geology. 2013. Vol. 359. P. 49–69.

Minyuk, P. S. and Borkhodoev, V. Ya. Geochemistry of Sediments from Lake Grand, Northeast Russia. Geochemistry International. 2016. Vol. 54 (9). P. 807–816.

Minyuk, P. S., Borkhodoev, V. Y., and Wennrich, V. Inorganic geochemistry data from Lake El'gygytgyn sediments: marine isotope stages 6-11. Climate of the Past. 2014. Vol. 10. P. 467–485.

Minyuk, P.S., Subbotnikova, T.V., and Plyashkevich, A.A. Measurements of Thermal Magnetic Susceptibility of Hematite and Goethite. Izvestiya, Physics of the Solid Earth. 2011. Vol. 47 (9). P. 762–774.

PALE, 1994. Research Protocols for PALE: Paleoclimates of Arctic Lakes and Estuaries. 53 pp. PAGES Workshop Report Series, Bern, Switzerland.

Petrovský, E. and Kapička, A. On determination of the Curie point from thermomagnetic curves. J. Geophys. Res. 2006. Vol. 111. B12S27, https://doi.org/10.1029/2006jb004507.

Ponomareva, V.V., Kyle, P.R., Melekestsev, I.V., Rinkleff, P.G., Dirksen, O.V., Sulerzhitsky, L. D., Zaretskaia, N.E., and Rourke, R., The 7600 (14C) Year BP Kurile Lake Caldera_Forming Eruption, Kamchatka, Russia: Stratigraphy and Field Relationships. J. Volcanol. Geotherm. Res. 2004. Vol. 136. P. 199–222.

Reimer, P.J., Bard, E., Bayliss, A., Beck, J.W., Blackwell, P.G., Bronch Ramsey, C., Buck, C.E., Cheng, H., Edwards, R.I., Friedrich, M., Grootes, P.M., Guilderson, T.P., Halidasson, H., Hajdas, I., Hatte, C., Heaton, T.J., Hoffman, D.I., Hogg, A.G., Hughen, K.A., Kaiser, K.F., Kromer, B., Manning, S.W., Niu, M., Reimer, R.W., Richards, D.A., Scott, E.M., Southon, J. R., Staff, R.A., Turney, C.A. & van der Plicht, J. IntCal13 and marine13 radiocarbon age calibration curves 0-50,000 years cal BP. Radiocarbon. 2013. Vol. 55. P. 1869–1887.

Sevast'tyanova, E. S. Behavior of phosphorus in oceanic ferromanganese micro and macronodules. Lithol. Polezn. Iskop. 1981. Vol. 6. P. 96–101 (in Russian).

Sevast'tyanova, E. S. Correlation of phosphorus and tetravalent manganese contents in pelagic oxidized clays. Okeanologiya. 1982. Vol. 32(6). P. 970–974 (in Russian).

Sharma, S., Joachimski, M., Sharma, M., Tobschall, H. J., Singh, I. B., Sharma, C., Chauhan, M. S., and Morgenroth, G. Late glacial and Holocene environmental changes in Ganga plain, Northern India. Quaternary Sci. Rev. 2004. Vol. 23. P. 145–159.

Song, J., Jia, S.-Y., Yu,B., Wu,S.-H., Han,X. Formation of iron (hydr)oxides during the abiotic oxidation of Fe(II) in the presence of arsenate. Journal of Hazardous Materials. 2015. Vol. 294. P. 70–79.

Webster, N.A.S., Loan, M.J., Madsen, I.C., Knott, R.B., Brodie, G. M., Kimpton, J. A. An in situ synchrotron X-ray diffraction investigation of lepidocrocite and ferrihydrite-seeded $Al(OH)_3$ crystallisation from supersaturated sodium aluminate liquor. Journal of Crystal Growth. 2012. Vol. 340. P. 112–117.

Wright, H.E., Jr., Mann, D.H., and Glaser, P.H. Piston Corers for Peat and Lake Sediments. Ecology. 1984. Vol. 65. P. 657–659.

Yudovich, Ya.E., Ketris, M.P. Geochemical indicators of Lithogenesis. (Ed. Tkachev Yu. A.). Syktytvkar, 2011. 742 p (in Russian).